Phys. Med. Biol. **54** (2009) 4561–4573 doi:10.1088/0031-9155/54/14/012

Induced current magnetic resonance electrical impedance tomography of brain tissues based on the J-substitution algorithm: a simulation study

Yang Liu[1], **Shanan Zhu**[1] **and Bin He**[2,3]

[1] College of Electrical Engineering, Zhejiang University, Hangzhou 310027, People's Republic of China

[2] Department of Biomedical Engineering, University of Minnesota, 7-105 NHH, 312 Church Street, Minneapolis, MN 55455, USA

E-mail: binhe@umn.edu

Received 4 October 2008, in final form 26 May 2009
Published 26 June 2009
Online at stacks.iop.org/PMB/54/4561

Abstract

We have investigated induced current magnetic resonance electrical impedance tomography (IC-MREIT) by means of computer simulations. The J-substitution algorithm was implemented to solve the IC-MREIT reconstruction problem. By providing physical insight into the charge accumulating on the interfaces, the convergence characteristics of the reconstruction algorithm were analyzed. The simulation results conducted on different objects were well correlated with the proposed theoretical analysis. The feasibility of IC-MREIT to reconstruct the conductivity distribution of head–brain tissues was also examined in computer simulations using a multi-compartment realistic head model. The present simulation results suggest that IC-MREIT may have the potential to become a useful conductivity imaging technique.

(Some figures in this article are in colour only in the electronic version)

1. Introduction

The recently introduced magnetic resonance electrical impedance tomography (MREIT) is an imaging technique that can noninvasively reconstruct the static image of a conductivity distribution within an object. In MREIT, a small current is injected into the object to be imaged through a pair of surface electrodes, and the magnetic flux density inside the object is measured by a MRI scanner. The current density distribution inside the object can then be obtained according to Ampere's law, $J = \frac{\nabla \times B}{\mu_0}$. The conductivity distribution can be reconstructed through the relation between the conductivity and either the magnetic flux density or the current density.

[3] Author to whom any correspondence should be addressed.

There has been considerable interest in MREIT in both theoretical and experimental studies. By minimizing the error between the measured and computed current densities, Kwon *et al* (2002) tried to reconstruct cross-sectional conductivity images. In that study, they also suggested that in order to reconstruct the absolute conductivity distribution, at least two current injection patterns were needed along with a single voltage measurement. Lee *et al* (2003) have successfully applied the J-substitution algorithm to data acquired from a saline phantom with a cylindrical sausage object inside. When a 28 mA current was injected, the relative L^2-error of the reconstructed image was 25.5%. Under the assumption of the measurement of the internal current density, an equipotential projection-based algorithm for anisotropic conductivity imaging was suggested by Değirmenci and Eyüboğlu (2007).

Both Seo *et al* (2003) and Oh *et al* (2003) used only one component of the measured magnetic flux density to reconstruct the conductivity distribution of a subject. Since both methods differentiate noisy Bz images twice, they are sensitive to measurement noise. Kim *et al* (2007) have successfully reconstructed the conductivity images of postmortem canine brains using a 3 T MREIT system with 40 mA imaging currents. In the most recent experimental study, they demonstrated the feasibility of MREIT to image the conductivity distribution of *in vivo* canine brains using 5 mA injection currents (Kim *et al* 2008). It was reported that the transversal J-substitution algorithm (Nam *et al* 2007) could considerably improve the quality of the reconstructed conductivity image under a low injection current. İder and Onart (2004) reported a new reconstruction algorithm by formulating the image reconstruction as the iterative solution of a nonlinear matrix equation. Gao *et al* used the MREIT algorithm to reconstruct the conductivity distribution of a piece-wise homogeneous realistic-geometry head model, based on the radial basis function network (Gao *et al* 2005a) and the response surface methodology (Gao *et al* 2006). Recently, Gao and He (2008) proposed a linear inverse solution of MREIT with a modified J-substitution algorithm.

As an alternative technique to MREIT, induced current magnetic resonance electrical impedance tomography (IC-MREIT) was proposed by Özparlak and İder (2005). In this technique, an eddy current is induced in the conductive object by the ac primary magnetic field. The secondary magnetic flux density produced by the eddy current can be measured by MRI and used to reconstruct the internal conductivity distribution. With IC-MREIT, Özparlak and İder (2005) reconstructed a conductivity image of the thorax using the algebraic algorithm.

Accurate human head conductivity imaging cannot only enhance the accuracy in EEG/MEG source localization (He 2004, 2005), but also has potential applications in the diagnosis of neurological diseases (Boone *et al* 1994, Holder 1992). In the present study, the J-substitution algorithm was applied to solve the IC-MREIT inverse problem. A series of computer simulations were conducted to evaluate the feasibility of the IC-MREIT technique to reconstruct the conductivity distribution of head–brain tissues.

2. Methods

2.1. The forward problem

Computation of the eddy current density and secondary magnetic flux density for a known conductivity distribution and boundary conditions is defined as the forward problem. Let Ω be a bounded and electrically conductive domain in R^3 with a boundary Γ. The conductivity distribution inside Ω is σ and assumed to be positive. Applying a low-frequency magnetic field, an eddy current can be induced in Ω. In an isotropic, linear and conductive medium, the sinusoidal electromagnetic field satisfies the following Poisson's equation and Neumann boundary conditions:

$$\nabla \cdot (\sigma \nabla \phi) = -j\omega \mathbf{A} \cdot \nabla \sigma \qquad \text{in} \qquad \Omega \tag{1}$$

$$\frac{\partial \phi}{\partial \mathbf{n}} = -j\omega \mathbf{A} \cdot \mathbf{n} \qquad \text{on} \qquad \Gamma, \tag{2}$$

where $\mathbf{n}$ is the unit outward normal vector, and ϕ and $\mathbf{A}$ are the electrical scalar potential and total magnetic vector potential in Ω, respectively. The electric field in Ω is given by

$$\mathbf{E} = -\nabla \phi - j\omega \mathbf{A}. \tag{3}$$

By recalling the fact that the secondary magnetic vector potential $\mathbf{A}_s$ due to the eddy current is much smaller than the primary magnetic vector potential $\mathbf{A}_p$ produced by the excitation coil (Gencer *et al* 1994, 1996), equations (1)–(3) can be reduced to

$$\nabla \cdot (\sigma \nabla \phi) = -j\omega \mathbf{A}_p \cdot \nabla \sigma \qquad \text{in} \qquad \Omega, \tag{4}$$

$$\frac{\partial \phi}{\partial \mathbf{n}} = -j\omega \mathbf{A}_p \cdot \mathbf{n} \qquad \text{on} \qquad \Gamma, \tag{5}$$

$$\mathbf{E} = -\nabla \phi - j\omega \mathbf{A}_p. \tag{6}$$

The eddy current density induced in the object can be calculated as

$$\mathbf{J}_e = \sigma \mathbf{E}. \tag{7}$$

If the phase of the ac current in the excitation coil is set as the reference phase (zero phase), $\mathbf{A}_p$ is purely real. Since σ is purely real, ϕ must be purely imaginary (Gencer *et al* 1994, Özparlak and İder 2005) and, consequently, it can be seen from equations (6) and (7) that $\mathbf{E}$ and $\mathbf{J}_e$ are also purely imaginary. From the Biot–Savart integral, the secondary magnetic flux density $\mathbf{B}_s$, due to $\mathbf{J}_e$, is

$$\mathbf{B}_s = \frac{\mu_0}{4\pi} \int_{\Omega} \mathbf{J}_e \times \frac{\mathbf{r} - \mathbf{r}'}{|\mathbf{r} - \mathbf{r}'|^3} \mathrm{d}v', \tag{8}$$

where $\mu_0 = 4\pi \times 10^{-7}\,\mathrm{H\,m^{-1}}$ is the permeability of free space, $\mathbf{r}$ and $\mathbf{r}'$ refer to field and source points defined in Ω, respectively. Since $\mathbf{J}_e$ is purely imaginary, $\mathbf{B}_s$ is also purely imaginary. The primary magnetic flux density $\mathbf{B}_p$ produced by the excitation coil is given by

$$\mathbf{B}_p = \frac{\mu_0}{4\pi} \int_{V} \mathbf{J} \times \frac{\mathbf{r} - \mathbf{r}'}{|\mathbf{r} - \mathbf{r}'|^3} \mathrm{d}v', \tag{9}$$

where $\mathbf{J}$ (purely real) is the source current density in the excitation coil. As analyzed above, $\mathbf{B}_p$ is purely real and $\mathbf{B}_s$ is purely imaginary. Namely, there is a 90° phase difference between them. Using the pulse sequence proposed by Özparlak and İder (2005), $\mathbf{B}_s$ can be measured by a MRI scanner. In the present study, the finite-element method (FEM) is adopted to solve the boundary value problem defined by equations (4) and (5).

2.2. *The inverse problem*

Given the measured secondary magnetic flux density or eddy current density, the calculation of the inner conductivity distribution is called the inverse problem of IC-MREIT. After a brief introduction of the J-substitution algorithm, which was originally proposed for MREIT (Kwon *et al* 2002), we will show that IC-MREIT can reconstruct the absolute conductivity distribution in an object without any boundary voltage measurement. The error function in J-substitution is defined as follows:

$$f(\sigma) = \int_{\Omega} ||\mathbf{J}^*| - \sigma|\mathbf{E}||^2 \mathrm{d}v', \tag{10}$$

where $|\mathbf{J}^*|$ is the magnitude of measured current density, and $|\mathbf{E}|$ is the magnitude of the calculated electric field when the conductivity is σ. Minimizing the above error function yields the updating strategy of conductivity:

$$\sigma = \frac{|\mathbf{J}^*|}{|\mathbf{E}|}. \tag{11}$$

In MREIT, if the injected current is kept the same, the internal current density distributions corresponding to two conductivity distributions, σ and $k\sigma$, where k is a constant, are the same (Kwon *et al* 2002, Birgül *et al* 2003). Accordingly, the conductivity distribution reconstructed from equation (11) differs from the true distribution by a scale factor. In order to image the absolute conductivity distribution, the boundary voltage data must be introduced into the update formula (Kwon *et al* 2002, İder *et al* 2003, Gao *et al* 2005b):

$$\sigma = \frac{|\mathbf{J}^*|}{|\mathbf{E}|}\frac{V_\sigma}{V_{\sigma^*}}, \tag{12}$$

where $V_{\sigma*}$ is the measured voltage difference, and V_σ is the calculated voltage difference when the conductivity is σ.

For IC-MREIT, the electric field $\mathbf{E}$ has two sources:

$$\mathbf{E}_{\mathrm{in}} = -j\omega\mathbf{A}_p, \tag{13}$$

$$\mathbf{E}_c = -\nabla\phi. \tag{14}$$

The induced electric field $\mathbf{E}_{\mathrm{in}}$ is due solely to the current flowing in the excitation coil. $\mathbf{E}_c$ is produced by the charge accumulating at the interface between two media with different conductivities. If the conductivity of the object increases k times, it can be seen from equations (4) and (5) that the electrical potential ϕ does not change. Since $\mathbf{E}_{\mathrm{in}}$ exists in the absence of the conductive object, the total electric fields corresponding to two conductivity distributions, σ and $k\sigma$, are the same, while the eddy current density corresponding to the latter is k times of the former. Therefore, IC-MREIT, unlike MREIT, can image the absolute conductivity distribution inside an object without any boundary voltage measurement.

2.3. Convergence characteristic of the IC-MREIT J-substitution algorithm

Suppose that the conductive object is composed of two media with different conductivities, σ_1 and σ_2, respectively. At the interface, the perpendicular component of the current density must be continuous:

$$\mathbf{J}_1 \cdot \mathbf{n} = \mathbf{J}_2 \cdot \mathbf{n}. \tag{15}$$

From equations (6) and (7), we get

$$\mathbf{J}_1 \cdot \mathbf{n} = -j\sigma_1\omega\mathbf{A}_{p1} \cdot \mathbf{n} - \sigma_1(\nabla\phi_1) \cdot \mathbf{n}, \tag{16}$$

$$\mathbf{J}_2 \cdot \mathbf{n} = -j\sigma_2\omega\mathbf{A}_{p2} \cdot \mathbf{n} - \sigma_2(\nabla\phi_2) \cdot \mathbf{n}. \tag{17}$$

Neglecting the secondary magnetic vector potential, we have $\mathbf{A}_{p1} = \mathbf{A}_{p2} = \mathbf{A}_p$. Equations (15)–(17) give

$$\sigma_1\left(\frac{\partial\phi_1}{\partial\mathbf{n}}\right) - \sigma_2\left(\frac{\partial\phi_2}{\partial\mathbf{n}}\right) = j(\sigma_2 - \sigma_1)\omega\mathbf{A}_p \cdot \mathbf{n}. \tag{18}$$

If the charge accumulating on the interface is not taken into account, the left-hand side of equation (18) is zero. Assuming that the primary magnetic vector potential $\mathbf{A}_p$ has the component perpendicular to the interface, the right-hand side of (18) is nonzero. It can be concluded that the continuous condition of the current density is satisfied because charge builds up on the interface. In the special case where the axis of the circular excitation coil passes through the center of a multiple-layer concentric sphere, no charge accumulates on the interface (Grandori and Ravazzani 1991, Roth *et al* 1991 and Tofts 1990). Then, the total electric field is equal to $\mathbf{E}_{\text{in}}$ and the magnitude of the eddy current density, $\mathbf{J} = \sigma\mathbf{E}_{\text{in}} = -j\sigma\omega\mathbf{A}_p$, is linear with σ. In this case, the IC-MREIT J-substitution algorithm converges to the true solution σ after the first iteration. If the component of $\mathbf{A}_p$ perpendicular to the interface is nonzero, charge builds up on the interface and $\mathbf{E}_c$ is no longer zero. The relation between the magnitude of $\mathbf{J}$ and σ is a rather severe nonlinear mapping. Therefore, multiple iterations are necessary to reconstruct the conductivity image of an object.

3. Computer simulation

In practice, the current density image is acquired from the measured magnetic flux density via Ampere's law. In the present simulation study, the 'measured' current density was simulated. Given the target conductivity distribution, through solving the forward problem, we can get the target current density. Various levels of random noise were then added to the target current density to simulate the 'measured' noise-contaminated current density, which was used to reconstruct the conductivity distribution inside the object based on the iterative J-substitution algorithm.

The present simulation study includes two parts. The objective of the first part, conducted on the two-sphere model and the prism model with sharp edges and corners, was to verify the theoretical studies given above. To test the feasibility of IC-MREIT to reconstruct the conductivity distribution of head–brain tissues, the second part of the simulation was conducted on the multi-compartment realistic head model. In the present study, the finite-element meshing and the forward problem solving were carried out using ANSYS 10.0.

3.1. Simulation conducted on the two-sphere and prism models

Since the aim of the first part of the simulation study was to verify the theoretical analysis, a one-coil IC-MREIT system was adopted and only the noise-free case was considered. We first carried out the numerical simulation on a two-sphere model. The inner sphere, 5 cm in radius, had a conductivity value of 5 S m^{-1}. The outer sphere, 10 cm in radius, had a conductivity value of 1 S m^{-1}. A 100-turn excitation coil with a 20 cm radius was concentric with the two-sphere model, as shown in figure 1. The excitation coil was driven by a 10 A current, with a 1 kHz frequency. The finite-element mesh of the two-sphere model contained 21 075 linear tetrahedral elements and 3788 nodes.

The correlation coefficient (CC) and relative error (RE) between the reconstructed and target conductivity distributions were used to quantitatively assess the performance of the IC-MREIT J-substitution algorithm. The CC and RE were defined as follows:

$$\mathrm{CC}[\sigma(i), \sigma^*(i)] = \frac{\sum_{i=1}^{N} \sigma(i) \cdot \sigma^*(i)}{\left[\sum_{i=1}^{N} \sigma^2(i)\right]^{1/2} \cdot \left[\sum_{i=1}^{N} \sigma^{*2}(i)\right]^{1/2}}, \tag{19}$$

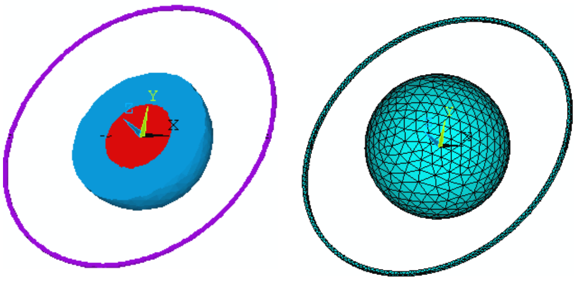

(a) (b)

Figure 1. (a) Cross-sectional image and (b) finite-element mesh of the two-sphere model with the excitation coil.

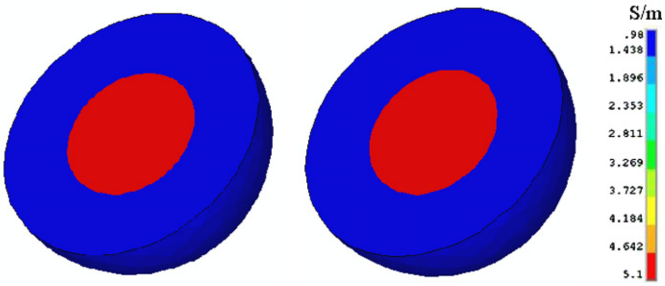

(a) (b)

Figure 2. (a) Target and (b) reconstructed conductivity distributions of the two-sphere model.

$$\mathrm{RE}[\sigma, \sigma^*] = \frac{\|\sigma^* - \sigma\|}{\|\sigma^*\|} \times 100\,\%, \tag{20}$$

where σ^* and σ are the target and reconstructed conductivity distributions, respectively.

The initial uniform conductivity distribution was taken to be 0.2 S m^{-1} and all of the following simulations began with this initial guess. After the first iteration, the CC and RE between the reconstructed and target conductivity distributions were 0.9999 and 0.1113%, respectively. The target and reconstructed conductivity cross-sectional images of the two-sphere model are shown in figure 2.

As we can see, when the excitation coil is concentric with the two-sphere model, $\mathbf{A}_p$ has no component perpendicular to the interfaces, and the magnitude of the eddy current is proportional to the conductivity. Therefore, we can reconstruct the conductivity image after the first iteration.

To verify that the IC-MREIT technique does not need any voltage measurement in the reconstruction of the absolute conductivity image, the distributions of the electric field magnitude and the eddy current density vector in the x–y plane for the two-sphere model are presented in figure 3. In the middle column, the conductivity of the inner sphere is set to 5 S m^{-1} and the conductivity of the outer sphere is set to 1 S m^{-1}. The conductivity values of the two-sphere model in the left and right columns are five times smaller and larger than that of the middle column, respectively. As we can see, the distributions of the electric field corresponding to three conductivity distributions are the same, while the magnitude of the eddy current density increases five times from left to right in each column. This result indicates

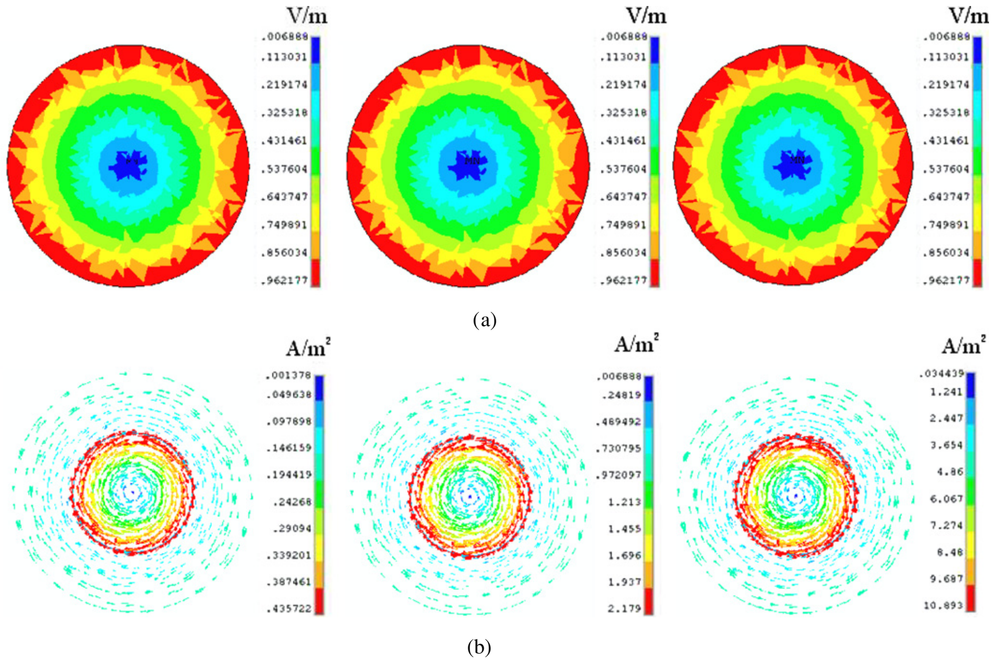

Figure 3. Distributions of (a) the electric field magnitude and (b) the eddy current density vector in the x–y plane for the two-sphere model.

that IC-MREIT is sensitive to the absolute conductivity within an object and does not need any boundary voltage measurement to reconstruct the absolute conductivity distribution.

In order to assess the convergence characteristic of the IC-MREIT J-substitution algorithm when $\mathbf{A}_p$ has a component perpendicular to the interfaces, the following numerical simulation was performed on a prism model. The conductivity of the inner regular triangular prism, 5 cm in length of each side, was set to 5 S m^{-1}. The conductivity of the outer regular quadrangular prism was set to 1 S m^{-1}. The length of each side on the top and bottom faces was 5 cm and the height was 10 cm. A 10 cm radius excitation coil was placed coaxially with the two prisms as shown in figure 4. The finite-element mesh of the prism model included 35 302 linear tetrahedral elements and 6442 nodes.

Figure 5 shows the target and reconstructed conductivity cross-sectional images of the prism model. It took 12 iterations to reconstruct this image. The CC and RE between the reconstructed and target conductivity distributions were 0.9980 and 6.3858%, respectively.

In this case, $\mathbf{A}_p$ is no longer parallel to the interfaces on which a large amount of charge builds up. This results in the nonlinear relationship between the magnitude of the eddy current density and the conductivity. Satisfactory reconstruction results can be achieved by multiple iterations.

In figure 6, the distributions of the electric field magnitude and the eddy current density vector in the x–y plane for the prism model corresponding to three conductivity distributions are illustrated. The conductivity values of the prism model in the left and right columns are five times smaller and larger than that of the middle column, respectively. The simulation results demonstrate that distributions of the electric field corresponding to three conductivity distributions are the same, while the magnitude of the eddy current density increases five

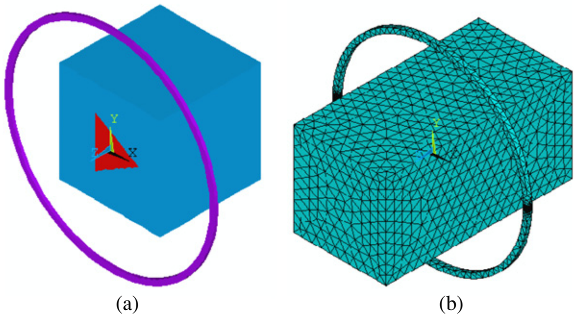

Figure 4. (a) Cross-sectional image and (b) finite-element mesh of the prism model with the excitation coil.

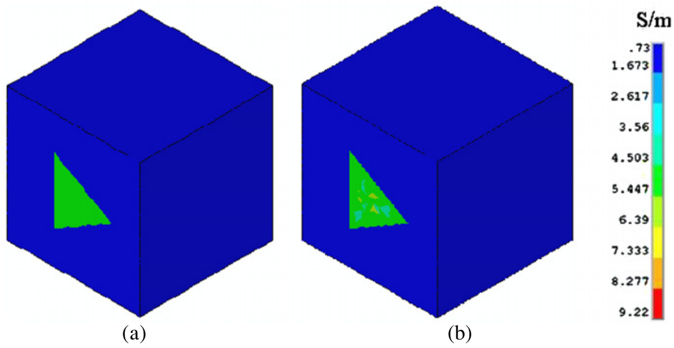

Figure 5. (a) Target and (b) reconstructed conductivity distributions of the prism model.

times from left to right in each column. The present simulation results provide a further confirmation that the IC-MREIT technique can reconstruct the absolute conductivity image without any voltage measurement.

3.2. Simulation conducted on a multiple-compartment realistic head model

In order to evaluate the feasibility of the IC-MREIT technique to reconstruct the human head conductivity distribution, a series of simulations were conducted on a realistic head model constructed from the MRI data of a human subject. This head model included five compartments: scalp, skull, cerebrospinal fluid (CSF), gray and white matter. We assigned the mean value from multiple references to the tissue conductivities: scalp at 0.33 S m^{-1}, skull at 0.0165 S m^{-1}, CSF at 1 S m^{-1}, gray at 0.276 S m^{-1} and white matter at 0.126 S m^{-1} (Zhang *et al* 2006a, 2006b , Wagner *et al* 2004). The finite-element mesh of the realistic head model, as shown in figure 7, contained 100 790 linear hexahedra elements and 108 953 nodes. Four circular coils, 18 cm in radii, were horizontally placed in the plane 6.5 cm below the vertex, and their centers were 3 cm away from the vertical axis of the head toward the anterior, posterior, left and right of the subject. A 35 A 1 kHz ac current was directed into each excitation coil in turn. The relative position of the first coil to the head is presented in figure 8.

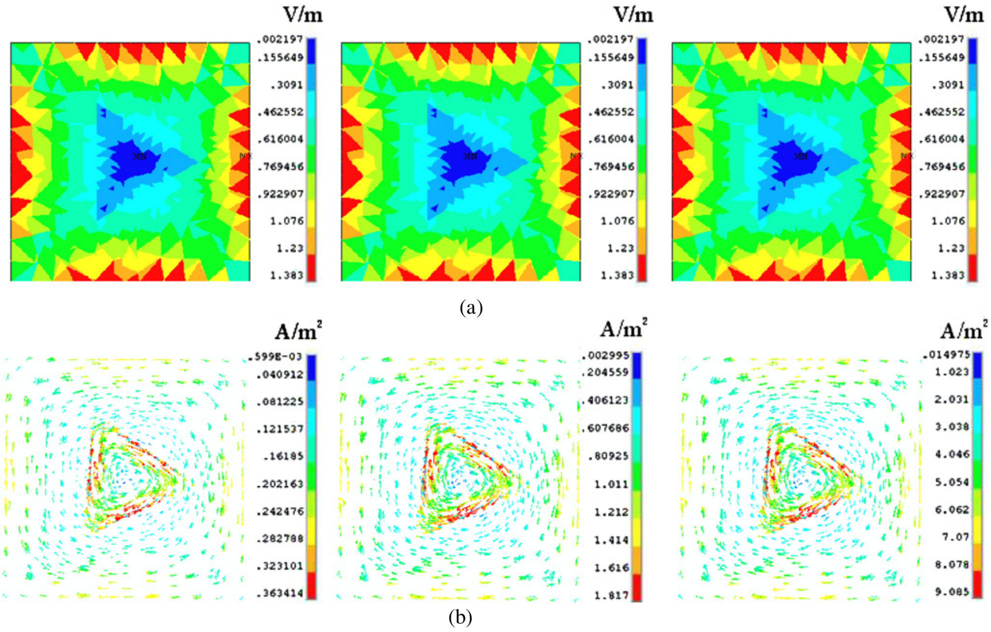

Figure 6. Distributions of (a) the electric field magnitude and (b) the eddy current vector in the x–y plane for the prism model.

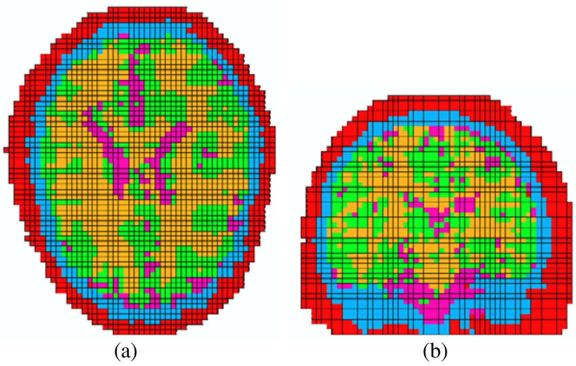

Figure 7. Finite-element meshes of the head model in (a) axial and (b) coronal view. The color labels correspond to red-scalp, blue-skull, purple-CSF, green–gray matter, yellow–white matter.

To examine the imaging quality at different levels of SNR, we added Gaussian random noise to the target current density. The standard deviations in J_x, J_y and J_z were given by Scott *et al* (1992) as

$$\sigma_{Jx} = \frac{1}{2\mu_0\gamma t_{\text{curr}}\text{SNR}}\sqrt{\left(\frac{F_y}{\Delta y}\right)^2 + \left(\frac{F_z}{\Delta z}\right)^2},$$

$$\sigma_{Jy} = \frac{1}{2\mu_0\gamma t_{\text{curr}}\text{SNR}}\sqrt{\left(\frac{F_x}{\Delta x}\right)^2 + \left(\frac{F_z}{\Delta z}\right)^2},$$

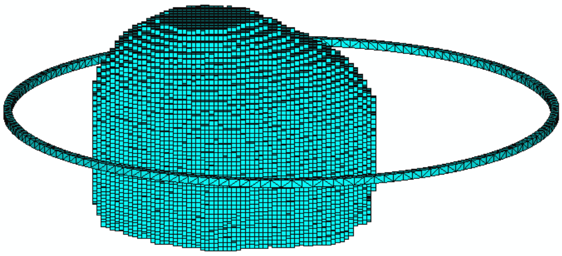

Figure 8. Relative position of the first coil to the head. The coil is placed in the plane 6.5 cm below the vertex and shifted 3 cm toward the anterior of the subject.

Table 1. Conductivity reconstruction results of the realistic head model.

	SNR = ∞	SNR = 200	SNR = 180	SNR = 150	SNR = 90
CC	0.9952	0.9879	0.9861	0.9835	0.9646
RE(%)	10.2645	16.7851	18.8368	22.8674	32.6328

$$\sigma_{Jz} = \frac{1}{2\mu_0\gamma t_{\text{curr}}\text{SNR}}\sqrt{\left(\frac{F_x}{\Delta x}\right)^2 + \left(\frac{F_y}{\Delta y}\right)^2},$$

where $\gamma = 26.75 \times 10^7$ rads^{-1} T^{-1} is the gyromagnetic ratio of hydrogen, $t_{\text{curr}} = 48$ ms is the duration of the applied current, SNR is the signal-to-noise ratio of the MR magnitude image, and $\Delta x = \Delta y = \Delta z = 3$ mm denote the voxel size. Provided that the 3×3 Sobel operators were used, $F_x = F_y = F_z = \frac{\sqrt{3}}{4}$. The standard deviations for SNR = 200, 180, 150 and 90 are 0.032 A m^{-2}, 0.035 A m^{-2}, 0.042 A m^{-2}, 0.070 A m^{-2}, respectively.

Table 1 lists the reconstruction results of the realistic head model at different SNR levels after six iterations. From these simulation results, we could see that the SNR of the MR magnitude images should be greater than 180 for achieving less than 20% relative error in reconstructed conductivity images. Since 200 SNR is possible for body coils and higher values can be obtained for head coils (Özparlak and İder 2005), IC-MREIT has promise in imaging the conductivity distribution of human head. Figure 9 shows the target and reconstructed conductivity distributions of the realistic head model in the plane of coils. It is shown that the IC-MREIT technique based on the J-substitution algorithm can accurately reconstruct the conductivity distribution of head–brain tissues for a SNR of infinity. Even with a SNR of 90, different types of brain tissues can be successfully distinguished.

4. Discussion

In the present study, the J-substitution algorithm (Kwon *et al* 2002) has been applied to solve the IC-MREIT (Özparlak and İder 2005) inverse problem. Using basic electromagnetic equations, we have shown that there is no need for voltage measurement in IC-MREIT to reconstruct the absolute conductivity distribution. Moreover, we have provided a physical insight into the charge accumulating on the interfaces, and suggest that both the relative position of the excitation coil to the object to be imaged and the medium distribution inside the object have significant effects on the convergence behavior of the reconstruction algorithm. The present simulation results obtained on a two-sphere model and a prism model provide a meaningful

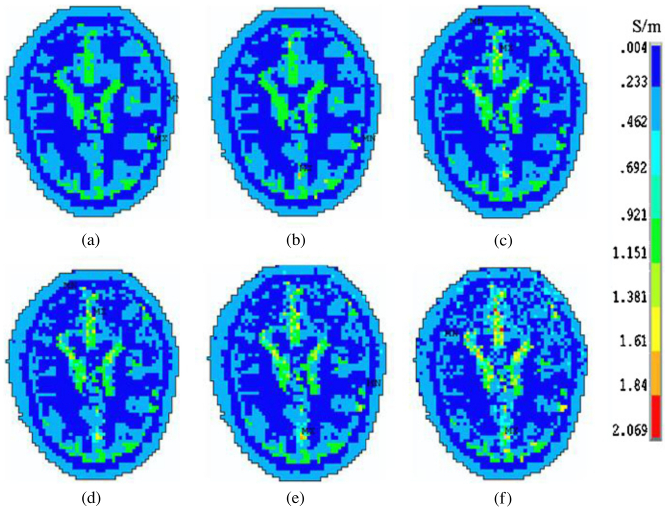

Figure 9. (a) Target and (b)–(f) reconstructed conductivity images of the realistic head model in the coil plane (6.5 cm below the vertex) corresponding to SNR = ∞, 200, 180, 150 and 90.

verification of the theoretical analysis. To test the feasibility of IC-MREIT to reconstruct the conductivity distribution of the head–brain tissues, computer simulations were conducted on a multiple-compartment realistic head model. The present simulation results suggest the potential capability of IC-MREIT to image the conductivity distribution of head–brain tissues.

Özparlak and İder (2005) suggested that since the combined system matrix is nonsingular, IC-MREIT can reconstruct the absolute conductivity image without the need for any additional peripheral voltage measurement. In the present study, we have derived this conclusion based on completely different and more straightforward grounds.

In clinical MR imaging, fast-switching gradients induce a time-varying electric field that may cause undesirable peripheral nerve stimulation (Vogt *et al* 2004, Schaefer *et al* 2000). According to IEC standard 60601–2-33, for the gradient system sinusoidally switched at a frequency of 1 kHz, the limits for the induced electric field in the normal operating mode and in the first-level controlled operating mode are 3.8 V m^{-1} and 4.7 V m^{-1}, respectively (Brand and Heid 2002). In the present simulation studies conducted on a multiple-compartment realistic head model, the maximum induced electric field and eddy current density were 8.98 V m^{-1} and 3.52 A m^{-2}, respectively. Since the induced electric field of 8.98 V m^{-1} is beyond the safety limit prescribed by the IEC standard, further efforts must be made to reduce the strength of the induced electric field. The number, position and size of the excitation coils should be optimized. Using an efficient denoising technique to preprocess the noisy magnetic flux density images will be also helpful.

In practice, some methods of effectively acquiring the secondary magnetic flux density should be further investigated. The approach presented by Gao and He (2008) can be used to overcome the rotation problem. In that approach, they first calculated the current density distribution from one component of the magnetic flux density, then reconstructed the conductivity image using the J-substitution algorithm. Other reconstruction algorithms based on one component of the magnetic flux density should be studied in the future.

It is worth noting that while the present simulation results are promising, the quality of the reconstructed image and the convergence rate of the IC-MREIT J-substitution algorithm depend on the coil configuration and conductivity distribution inside the object. We will work on a method to overcome this adverse sensitivity.

In summary, we applied the J-substitution algorithm to solve the IC-MREIT reconstruction problem, and verified in a straightforward manner that IC-MREIT could reconstruct the absolute conductivity distribution without the need for any boundary voltage measurement. In addition, the convergence characteristics of the reconstruction algorithm were analyzed by providing insight into the charge accumulating on the interfaces. The simulation results performed on the realistic head model demonstrated the potential feasibility of IC-MREIT in reconstructing the conductivity distributions of head–brain tissues, which may provide an important alternative to noninvasive conductivity imaging of the human head.

Acknowledgments

The authors would like to thank Dandan Yan and Xiaotong Zhang for helpful discussions. This work was supported in part by NSFC 5057705, NSF BES-0602957, NIH R21006070 and R01EB007920.

References

Birgül Ö, Eyüboğlu B M and İder Y Z 2003 Current constrained voltage scaled reconstruction (CCVSR) algorithm for MR-EIT and its performance with different probing current patterns *Phys. Med. Biol.* **48** 653–71

Boone K, Lewis A M and Holder D S 1994 Imaging of cortical spreading depression by EIT: implications for localization of epileptic foci *Physiol. Meas.* **15** A189–98

Brand M and Heid O 2002 Induction of electric fields due to gradient switching: a numerical approach *Magn. Reson. Med.* **48** 731–4

Değirmenci E and Eyüboğlu B M 2007 Anisotropic conductivity imaging with MREIT using equipotential projection algorithm *Phys. Med. Biol.* **52** 7229–42

Gao N and He B 2008 Noninvasive imaging of bioimpedance distribution by means of current reconstruction magnetic resonance electrical impedance tomography *IEEE Trans. Biomed. Eng.* **55** 1530–8

Gao N, Zhu S A and He B 2005a Estimation of electrical conductivity distribution within the human head from magnetic flux density measurement *Phys. Med. Biol.* **50** 2675–87

Gao N, Zhu S A and He B 2005b Use of 3-D magnetic resonance electrical impedance tomography in detecting human cerebral stroke: a simulation study *J. Zhejiang Univ. Sci.* B **6** 438–45

Gao N, Zhu S A and He B 2006 A new magnetic resonance electrical impedance tomography (MREIT) algorithm: the RSM-MREIT algorithm with applications to estimation of human head conductivity *Phys. Med. Biol.* **51** 3067–83

Gencer N G, İder Y Z and Williamson S J 1996 Electrical impedance tomography: induced-current imaging achieved with a multiple coil system *IEEE Trans. Biomed. Eng.* **43** 139–49

Gencer N G, Kuzuoğlu M and İder Y Z 1994 Electrical impedance tomography using induced currents *IEEE Trans. Med. Imaging* **13** 338–50

Grandori F and Ravazzani P 1991 Magnetic stimulation of the motor cortex-theoretical considerations *IEEE Trans. Biomed. Eng.* **38** 180–91

He B 2004 *Modeling and Imaging of Bioelectrical Activity—Principles and Applications* (Dordrecht: Kluwer)

He B 2005 *Neural Engineering* (Dordrecht: Kluwer)

Holder D S 1992 Detection of cerebral ischaemia in the anaesthetized rat by impedance measurement with scalp electrodes: implications for non-invasive imaging for stroke by electrical impedance tomography *Clin. Phys. Physiol. Meas.* **13** 63–75

İder Y Z and Onart S 2004 Algebraic reconstruction for 3D magnetic resonance-electrical impedance tomography (MREIT) using one component of magnetic flux density *Physiol. Meas.* **25** 281–94

İder Y Z, Onart S and Lionheart W R B 2003 Uniqueness and reconstruction in magnetic resonance-electrical impedance tomography (MR-EIT) *Physiol. Meas.* **24** 591–604

Kim H J *et al* 2008 *In vivo* electrical conductivity imaging of a canine brain using a 3 T MREIT system *Physiol. Meas.* **29** 1145–55

Kim H J, Lee B I, Cho Y, Kim Y T, Kang B T, Park H M, Lee S Y, Seo J K and Woo E J 2007 Conductivity imaging of canine brain using a 3 T MREIT system: postmortem experiments *Physiol. Meas.* **28** 1341–53

Kwon O, Woo E J, Yoon J R and Seo J K 2002 Magnetic resonance electrical impedance tomography (MREIT): simulation study of J-substitution algorithm *IEEE Trans. Biomed. Eng.* **49** 160–7

Lee B I, Oh S H, Woo E J, Lee S Y, Cho M H, Kwon O, Seo J K and Baek W S 2003 Static resistivity image of a cubic saline phantom in magnetic resonance electrical impedance tomography (MREIT) *Physiol. Meas.* **24** 579–89

Nam H S, Lee B I, Choi J, Park C and Kwon O I 2007 Conductivity imaging with low level current injection using transversal *J*-substitution algorithm in MREIT *Phys. Med. Biol.* **52** 6717–30

Oh S H, Lee B I, Woo E J, Lee S Y, Cho M H, Kwon O and Seo K J 2003 Conductivity and current density image reconstruction using harmonic Bz algorithm in magnetic resonance electrical impedance tomography *Phys. Med. Biol.* **48** 3101–16

Özparlak L and İder Y Z 2005 Induced current magnetic resonance-electrical impedance tomography *Physiol. Meas.* **26** S289–305

Roth B J, Saypol J M, Hallert M and Cohen L G 1991 A theoretical calculation of the electric field induced in the cortex during magnetic stimulation *Electroencephalogr. Clin. Neuronphysiol.* **81** 47–56

Schaefer D J, Bourland J D and Nyenhuis J A 2000 Review of patient safety in time-varying gradient fields *J. Magn. Reson. Imaging* **12** 20–9

Scott G C, Joy M L G, Armstrong R L and Henkelman R M 1992 Sensitivity of magnetic-resonance current-density imaging *J. Magn. Reson.* **97** 235–54

Seo J K, Yoon J R, Woo E J and Kwon O 2003 Reconstruction of conductivity and current density images using only one component of magnetic field measurements *IEEE Trans. Biomed. Eng.* **50** 1121–4

Tofts P S 1990 The distribution of induced currents in magnetic stimulation of the nervous system *Phys. Med. Biol.* **35** 1119–28

Vogt F M, Ladd M E, Hunold P, Mateisescu S, Hebrank F X, Zhang A, Debatin J F and Göhde S C 2004 Increased time rate of change of gradient fields: effect on peripheral nerve stimulation at clinical MR imaging *Radiology* **233** 548–54

Wagner T A, Zahn M, Grodzinsky A J and Pascual-Leone A 2004 Three-dimensional head model simulation of transcranial magnetic stimulation *IEEE Trans. Biomed. Eng.* **51** 1586–98

Zhang Y C, Ding L, Drongelen W V, Hecox K, Frim D M and He B 2006a A cortical potential imaging study from simultaneous extra- and intracranial electrical recordings by means of the finite element method *Neuroimage* **31** 1513–24

Zhang Y C, van Drongelen W and He B 2006b Estimation of *in vivo* human brain-to-skull conductivity ratio with the aid of intracranial electrical simulation *Appl. Phys. Lett.* **89** 223903